Enhancement of parity violating mixing in halo nuclei and the problem of neutron weak parity nonconserving potential constant

M.S. Hussein†, A.F.R. de Toledo Piza†, O.K. Vorov† and A.K. Kerman*
† *Instituto de Fisica,*
Universidade de Sao Paulo ,
Caixa Postal 66318, 05315-970,
Sao Paulo, SP, Brasil
* *Center for Theoretical Physics,*
Laboratory for Nuclear Science and Department of Physics,
Massachusetts Institute of Technology,
Cambridge, Massachusetts 02139, USA
(15 Yuly 1999)

arXiv:nucl-th/9908047v2 13 Aug 1999

Abstract

We consider the Parity Nonconserving (PNC) mixing in the ground state of exotic (halo) nuclei caused by the PNC weak interaction between outer neutron and nucleons *within nuclear interior*. For the nucleus ^{11}Be as an example of typical nucleus with neutron halo, we use analytical model for the external neutron wave functions to estimate the scale of the PNC mixing. The amplitude of the PNC mixing in halo state is found to be an order of magnitude bigger than that of typical PNC mixing between the "normal" nuclear states in nearby nuclei. The enhanced PNC mixing in halo cloud is proportional to the neutron weak PNC potential constant g_n^W only.

PACS: 24.60.Dr, 25.40.Dn

Typeset using REVTEX

I. INTRODUCTION

The parity nonconserving (PNC) nucleon interaction in nuclei caused by the PNC Weak interaction, and PNC effects in neutron-nucleus reactions are subject of current interest for both experimentalists and theorists [1–9]. The overall scale of the observable PNC effects is found to be in reasonable agreement with estimates in existing theory of the weak interactions [1] based on the Standard Model. Complete understanding of PNC forces in nuclear domain, which requires reliable QCD-based models of hadrons is far from being reached. This motivates extensive studies of the strengths of the PNC forces.

So far, the PNC effects have been probed in "normal" nuclei. Physics of "exotic" nuclei studied with unstable nuclear beams [10–22] appears to be one of the most promising modern nuclear areas. Due to their specific structure, exotic nuclei, e.g., halo nuclei can offer new possibilities to probe those aspects of nuclear interactions which are not accessible with normal nuclei. It is therefore interesting to examine possibilities of using exotic nuclei to investigate the effects of violation of fundamental symmetries, i.e., spatial parity and time reversal.

Some aspects of the Weak interactions in exotic nuclei have been discussed in literature [17], [18] in relation to the beta decay and to possibilities to study the parameters of the Cabibbo-Kobayashi-Mascawa matrix. To the best of our knowledge, however, the issue of the PNC effects in exotic nuclei has not been addressed yet.

The aim of this work is to present a first evaluation of the magnitude of the PNC effects in halo nuclei. We confine ourselves to the case of nucleus ^{11}Be, the most well studied, both experimentally and theoretically [10–12], [15], [16] . We find that the ground state, the $2s_{1/2}$ halo configuration, acquires admixture of the closest in energy halo state of opposite parity, $1p_{1/2}$. This effect originates from the weak interaction of the external halo neutron with the core nucleons in the nuclear interior. As a result, the neutron halo cloud surrounding the nucleus acquires the wrong parity admixtures that may be tested in experiments which can probe the halo wave functions in the exterior.

The magnitude of the admixture is found to be $\sim 10^{-6} \times g_n^W$ that is an order of magnitude bigger than the PNC effects in normal spherical nuclei. What is important to notice is that the enhanced effect we have found here is proportional to the *neutron weak constant* g_n^W only. The value of this constant remains to be one of the most questionable points in modern theory of parity violation in nuclear forces [5]. The enhanced PNC mixing in halo found here can be therefore useful in studies of the neutron weak constant.

One should mention another interesting question related to the structure of the PNC force in nucleus, namely, the strength of the isovector P-odd potential that has been discussed in Refs. [6,7].

In the next two sections, we recall the basic facts about the PNC weak interaction between nucleons starting from the Hamiltonian of Desplanques, Donoghue and Holstein (DDH). We consider the potential approximation to relate the parameters of the initial PNC Hamiltonian to the single-particle PNC mixing effects in nuclei, and discuss the problem of the neutron PNC constant in Sec.III. In Sec.IV, we analyze the basic effects of the halo structure on the magnitude of the single-particle PNC mixing and make estimates. In Sec.V, we use analytical approximation for the halo wave functions in ^{11}Be to calculate the matrix elements of the PNC weak interaction involving halo states and to estimate the

magnitude of PNC mixing in the ground state. Sec.VI summarizes the results and presents brief discussion of their implications.

II. WEAK NUCLEON-NUCLEON INTERACTION AND PARITY VIOLATING EFFECTS. POTENTIAL APPROXIMATION

We start with writing the nuclear Hamiltonian H in the form

$$H = H_S^0 \quad + \quad V_S^{res} \quad + \quad W^{PNC} \quad , \tag{1}$$

where the first term $H_S^0 = \sum_a (\vec{p_a}^{\,2}/2m + U_S(r_a))$ is the single particle Hamiltonian of the nucleons including the single-particle piece U_S of the strong interaction, V_S^{res} is the residual two-body strong interaction. The last term, W^{PNC} is the PNC part of the Weak interaction that is the source of the PNC effects.

The magnitude of the PNC effects is sensitive to both the weak PNC interaction matrix elements between the states of opposite parity and to the nuclear structure effects given by the strong part of the Hamiltonian (1). The latter one is invariant under spatial coordinate reflections, and if there is no weak interaction term W^{PNC} in (1), and as such parity is preserved, the eigenstates $|\Psi_s\rangle$ of the strong Hamiltonian $H_S^0 + V_S^{res}$ with energies E_s can be labeled by the parity quantum number (positive or negative), $|\Psi_s^+\rangle$, $|\Psi_s^-\rangle$. Due to presense of PNC weak interaction W^{PNC} in the nuclear Hamiltonian (1), a state of definite parity, say, $|\Psi_s^+\rangle$, acquires very small admixtures of wrong parity configurations. This can be accounted for by using the first order of perturbation theory with respect to W^{PNC}:

$$|\Psi_s^+\rangle' = |\Psi_s^+\rangle + \sum_{s1} \frac{\langle \Psi_{s1}^- | W^{PNC} | \Psi_s^+ \rangle}{E_s - E_{s1}} |\Psi_{s1}^-\rangle. \tag{2}$$

Here, prime denotes the corrected wave function that accounts for the PNC interaction and sum goes over available states of opposite parity, $|\Psi_{s1}^-\rangle$. The magnitude of measurable PNC effects is normally proportional to the coefficients f^{PNC} [2] that determine the dominating admixtures of the wrong parity states

$$f = \frac{\langle \Psi_{s1}^- | W^{PNC} | \Psi_s^+ \rangle}{\Delta E}. \tag{3}$$

The natural scale of the PNC effects in nuclei under usual conditions is [1], [2]

$$|f| \simeq 10^{-7} \tag{4}$$

that is roughly the ratio of the strength of the Weak PNC forces (matrix element in the numerator of (3)) and the strength of the strong interaction (energy denominator in (3)). In highly selective experiments, the PNC effects can be enhanced considerably as compared to estimate (4), due to specific properties of a specially chosen nuclear system or process. To reach high sensitivity to the wrong parity admixtures, one usually seeks possibilities to have the denominator ΔE in (3) minimal while keeping the PNC matrix element at maximum and to improve selectivity of measurable effect. This is typical for any tests of fundamental symmetries.

The most widely used version of the microscopic PNC interaction is the DDH Hamiltonian W_{DDH}^{PNC} [1], where the PNC forces are mediated by mesons. Its form stems from the analysis of interactions between intranucleon quarks via exchange of heavy bosons of Standard Model. The nonrelativistic P-odd weak interaction between nucleons approximated by the one-meson exchange can be written in the form [2], [1]

$$W_{DDH}^{PNC} = i\frac{h_\pi^{(1)} g_\pi}{4\sqrt{2}m}(\vec{\tau}_1 \times \vec{\tau}_2)^{(3)}(\vec{\sigma}_1 + \vec{\sigma}_2)[\vec{p}_1 - \vec{p}_2, \mathcal{F}_\pi] - \\ -\frac{g_\rho h_\rho^0}{2m}(\vec{\tau}_1 \cdot \vec{\tau}_2)(\vec{\sigma}_1 - \vec{\sigma}_2)\{\vec{p}_1 - \vec{p}_2, \mathcal{F}_\rho\} - \\ -\frac{g_\rho h_\rho^0}{2m} i(1+\mu)(\vec{\tau}_1 \cdot \vec{\tau}_2)(\vec{\sigma}_1 \times \vec{\sigma}_2)[\vec{p}_1 - \vec{p}_2, \mathcal{F}_\rho\} + W', \tag{5}$$

where the standard notations $\mathcal{F}_{\pi(\rho)} = \frac{e^{-m_{\pi(\rho)}|\vec{r}_1 - \vec{r}_2|}}{4\pi|\vec{r}_1 - \vec{r}_2|}$ are used and $[.,.]$ and $\{.,.\}$ denote the commutator and anticommutator, respectively. The subscripts 1 and 2 label the interacting nucleons, the superscript (3) denotes the third isospin projection. Here, m, m_π and m_ρ are the masses of the nucleon, π- and ρ-meson, respectively; σ (τ) stand for the spin (isospin) Pauli matrices, $\mu = 3.7$ is the isovector part of the anomalous magnetic moment of nucleon. W' denotes contributions from heavier mesons, which are less important. The values of the corresponding weak and strong coupling constants $h_\pi^{(1)}$, g_π, g_ρ, and h_ρ^0 can be found in [1], [2].

In nuclear environment, a nucleon experiences the combined action of the PNC forces (5) from other nucleons. It is known, see, e.g., [2], that the most of P-odd effects caused by the weak interaction W_{DDH}^{PNC} (5) in (1) can be successfully modeled by introducing the effective one-body P-odd interaction, or the "weak potential", W_{sp}, acting on the nucleon 1 as a single-particle operator which arises from averaging W^{PNC} over the states of other nucleons $W_{sp} \equiv \langle W^{PNC} \rangle$. Within this approximation, the Hamiltonian of the weak interaction in a nucleus takes particularly simple form of a sum of the proton W_{sp}^p and neutron W_{sp}^n symmetry violating potentials

$$W_{sp} = W_{sp}^p + W_{sp}^n = g_p^W \frac{G}{2\sqrt{2}m}\{(\vec{\sigma}_p \vec{p}_p), \rho\} + g_n^W \frac{G}{2\sqrt{2}m}\{(\vec{\sigma}_n \vec{p}_n), \rho\}, \tag{6}$$

where $G = 10^{-5} m^{-2}$ is the Fermi constant, $\vec{p}_{p(n)}$ and $\vec{\sigma}_{p(n)}$ refer to the proton (neutron) momentum and doubled spin respectively. The coherent contribution from all the occupied nucleon orbitals composing the core yields the nuclear density $\rho = \sum_{occ} |\psi_{occ}|^2$ in the expression (6). The dimensionless constants g_p^W and g_n^W of order of unity, for the proton and neutron potentials, are related to the parameters of the DDH Hamiltonian and depend on nuclear charge and neutron number. The single-particle approximation (6) for the PNC weak interaction (5) turns out to be very accurate [2]. It works satisfactorily even in the case of compound nuclear states [4], [25–27] where (6) gives the dominating contribution [25], [26] despite the fact that the wave functions are of essentially many-body nature.

III. PROTON AND NEUTRON WEAK POTENTIAL STRENGTHS

The knowledge about the proton and neutron constants g_p^W and g_n^W accumulated to date can be summarized as follows:

$$g_p^W = 4.5 \pm 2, \qquad g_n^W = 1 \pm 1.5. \tag{7}$$

These widely used values [2,5,24,25] correspond to the best values [1] of the microscopic parameters in the DDH Hamiltonian (5) and they are found in reasonable agreement with the bulk experimental data on parity violation, including the recent compound nuclear experiments [3] and anapole moment measurements [31]. The above relatively small absolute value of the neutron constant that follows from DDH analysis, results basically from cancellation between π- and ρ-meson contributions to g_n^W, while both mesons contribute coherently to the proton constant g_p^W, see, e.g. [5]. Due to this difference between the absolute values of the proton and neutron constants, the proton constant tends to dominate most measurable PNC effects [23,24,28,29], especially when both g_p^W and g_n^W can contribute. In some cases (such as odd proton nuclei), the contribution from the neutron constant, g_n^W, is suppressed irrespectively of its strength [2], [6]. In this sense, one usually measures the value of g_p^W, and it is difficult to probe g_n^W unless special suppression of the proton contribution occurs, and/or contribution of g_n^W is highlighted. By contrast, the case we consider in this work is sensitive to the value of the neutron constant only.

IV. HALO STRUCTURE EFFECTS ON THE PNC MIXING

The basic specific properties of the halo nuclei are determined by the fact of existence of loosely bound nucleon in addition to the core composed by the rest of the nucleons [13] (we will be interested here in the most well studied case of neutron halo). The matter distribution is shown schematically in Fig.1 (part a).

In one-body halo nuclei like ^{11}Be, the ground state is particularly simple: it can be represented as direct product of the single-particle wave function of the external neutron, ψ_{halo}, and the wave function of the core. The residual interaction V_S^{res} in (1) can be neglected as the many-body effects related to the core excitations are generically weak in such nuclei [33]. The problem with the Hamiltonian (1) is reduced to a single-particle problem for the external nucleon. The PNC potential matrix element between the ground state of halo nucleus and a state with opposite parity is

$$\langle \psi_{halo}^+ | W^{PNC} | \psi_{halo}^- \rangle = g_n^W \frac{G}{2\sqrt{2}m} \langle \psi_{halo}^+ | \{ (\vec{\sigma}_n \vec{p}_n), \rho_c \} | \psi_{halo}^- \rangle, \tag{8}$$

where $\rho_c(r)$ is the core density. Due to relatively heavy core for $A \simeq 10$, difference between the center of mass coordinate and the center of core coordinate can also be neglected.

The effective potential that binds external neutron is rather shallow yielding small single-neutron separation energy, and one can expect small energy spacing between the opposite parity states. The PNC effects (3), (2) can therefore be considerably magnified. The spectrum of ^{11}Be is shown in Fig.1(b). To evaluate the PNC mixing f^{HALO} in the ground state of this nucleus, it is enough to know the single-particle matrix element between the ground state 2s and the nearest opposite parity state 1p, and use their energy separation that is known experimentally.

The second effect of halo is that the value of the matrix element of the operator (6) between the halo states can be dramatically reduced as compared to its value in the case of "normal" nuclear states. The single-particle weak PNC potential (6) in (8) originates from

the DDH Hamiltonian (5) which is two-body operator, this fact is hidden in the nucleon density of the core $\rho_c(r)$. The external neutron spends most of its time away from the core region where only it can experience the PNC potential created by the rest of nucleons. Indeed, the dominant contribution to the matrix element of (6) between the halo states in (8) must come from the regions where the three functions can overlap coherently: $\psi^+_{halo}(r)$, $\psi^-_{halo}(r)$ and the core density $\rho_{core}(r)$. The latter one is essentially restricted by the region of nuclear interior, $r < r_c$ thus reducing the effective volume of required interference region to $\frac{4}{3}\pi r_c^3$. Normalization condition implies that the extended wave function of the bound state halo $\psi^{\pm}_{halo}(r)$ must be considerably reduced in the volume of coherent overlap $\frac{4}{3}\pi r_c^3$. By contrast, in "normal" nuclei the radii of localization of the wave functions with opposite parity that can be mixed by the weak interaction coincide generically with the core radius r_c. The resulting suppression for the PNC halo matrix element $\langle\psi^-_{halo}(r)|W_{sp}|\psi^+_{halo}(r)\rangle$ with respect to the matrix element for the normal nuclei can be extracted from the following simple estimate

$$\frac{\langle\psi^-_{halo}|W_{sp}|\psi^+_{halo}\rangle}{\langle\psi^-_{normal}|W_{sp}|\psi^+_{normal}\rangle} \sim \left(\frac{r_c}{r_{halo}}\right)^3 \sim \left(\frac{2fm}{6fm}\right)^3 \sim \frac{1}{25}...\frac{1}{30} \tag{9}$$

where we have used the mean square radii of halos from Ref. [12]. This suppression factor can cancel out the effect of the small energy separation (the denominator in Eq.(3)) and to suppress the PNC effects. This simple estimate does not account for the structure of the halo wave functions which can be quite substantial and may even lead to further suppression in the PNC mixing. In the following, we present a detailed analysis of the related effects. In particular, we find that the crude estimate (9) turns out rather pessimistic.

V. HALO MODEL AND EVALUATION OF THE PNC MIXING IN THE GROUND STATE OF ^{11}BE

The form of the single-particle wave functions of halo states can be deduced from their basic properties [16] and their quantum numbers [12]. The results of the Hartree-Fock calculations which reproduce the main halo properties (e.g., mean square radii) are also available [12]. We use the following ansatz for the model wave function of the $2s$ halo state:

$$\psi_{2s} = R_{2s}(r)\Omega^{l=0}_{j=1/2,m}, \quad R_{2s}(r) = C_0(1-(r/a)^2)exp(-r/r_0) \tag{10}$$

Here, $R_{2s}(r)$ is the radial part of the halo wave function and $\Omega^{l=0}_{j=1/2,m}$ is the spherical spinor. As we can neglect the center of mass effect for the heavy ($A = 10$) core, the halo neutron coordinate r in $R_{2s}(r) = \frac{1}{r}\chi_{2s}(r)$ is reckoned from the center of nucleus. The constant C_0 is determined from the normalization condition, $\int\limits_0^\infty dr[\chi_{2s}(r)]^2 = 1$ (we choose the radial wave functions to be real). We have

$$C_0 = \frac{2^{3/2}a^2}{r_0^{3/2}\sqrt{45r_0^4 + 2a^4 - 12a^2r_0^2}} \tag{11}$$

The parameters r_0 and the a are the corresponding lengths to fit the density distributions obtained in Ref. [12] and the mean square radius. The value of a is practically fixed to be $a = 2fm$ what corresponds to the position of the node. Recently, the node position have been restored from the analysis of the scattering process in work [16].

For the wave function $\psi_{1p} = R_{1p}(r)\Omega^{l=1}_{j=1/2,m}$ of the excited state $1p$, the following simplest form of the radial wave function turns out to be adequate

$$R_{1p}(r) = C_1 r exp(-r/r_1), \tag{12}$$

where C_1 is the normalization constant $C_1 = \frac{2}{\sqrt{3}} r_1^{-5/2}$ and the only tunable parameter r_1 is related to the $1p$ halo radius. The mean square root radii for the halo wave states (10) and (12) are given by

$$\sqrt{\langle r^2_{2s}\rangle} = r_0 \left(\frac{6(45r_0^4 + 2a^4 - 12a^2r_0^2)}{105r_0^4 + a^4 - 15a^2r_0^2}\right)^{1/2}, \quad \sqrt{\langle r^2_{1p}\rangle} = \left(\frac{15}{2}\right)^{1/2} r_1. \tag{13}$$

The matrix element of the weak interaction (6),(8) between the ground state and the first excited state reads

$$\langle 2s|W_{sp}|1p\rangle = \tag{14}$$
$$ig_n^W \frac{G}{\sqrt{2}m} \int_0^\infty dr \chi_{2s}(r) \left(\rho_c(r)\frac{d}{dr} + \frac{\rho_c(r)}{r} + \frac{1}{2}\frac{d\rho_c(r)}{dr}\right)\chi_{1p}(r)$$

The core nucleon density $\rho_c(r)$ has been tuned to reproduce the data obtained from Ref. [12]. We found that their results are excellently reproduced by the Gaussian-shaped ansatz $\rho_c(r)$,

$$\rho_c(r) = \rho_0 e^{-(r/R_c)^2} \tag{15}$$

with the values of the parameters $\rho_0 = 0.2fm^{-3}$ and $R_c = 2fm$, as shown on Fig.2.

Using the model wave functions (10),(10) and the core density (15), the required integrals can be done analytically, and we arrive with the result

$$\langle 2s|W|1p\rangle = ig_n^W \frac{G}{\sqrt{2}m}\mathcal{R} \tag{16}$$

where

$$\mathcal{R} = \rho_0 R_c^3 C_0 C_1 \Big\{ 3I_2(y) - \left[3\left(\frac{R_c}{a}\right)^2 + 1\right] I_4(y) +$$
$$+ \left(\frac{R_c}{a}\right)^2 I_6(y) - \frac{R_c}{r_1}\left[I_3(y) - \left(\frac{R_c}{a}\right)^2 I_5(y)\right]\Big\} \tag{17}$$

where $y = \frac{R_c(r_0+r_1)}{r_0 r_1}$ and the functions I_n are given by

$$I_n(y) = \int_0^\infty dx \quad x^n e^{-x^2-yx} = (-1)^n \frac{\sqrt{\pi}}{2}\frac{d^n}{dy^n} e^{y^2/4} erfc(y/2),$$

where $erfc(y)$ is the error function

$$erfc(y) = 1 - \frac{2}{\sqrt{\pi}} \int_0^y dt \quad exp(-t^2/2).$$

To obtain the results for the PNC weak interaction matrix element, we used the parameters r_0 and r_1 in the halo wave functions to fit the radial densities of the halos obtained by Sagawa [12].

The results for the best parameters are shown in Figs. 3 and 4 for the $2s$ and the $1p$ halos, respectively. One sees that the agreement for the densities is very good. Below, we use the values

$$\begin{aligned} r_0(best \quad value) &= 1.45 fm, \\ r_1(best \quad value) &= 1.80 fm, \end{aligned} \tag{18}$$

to calculate the matrix elements in Eqs. (14,16, 17). The radial wave functions χ are given in Fig.5. We used also deviations of the both r_0 and r_1 from (18) to check robustness of the results with respect to variations in the halo structure details. The values of the halo radii given by (13), $\sqrt{\langle r_{2s}^2 \rangle} = 5.9 fm$ and $\sqrt{\langle r_{1p}^2 \rangle} = 4.9 fm$ are close to the values of Ref. [12] $6.5 fm$ and $5.9 fm$ which agree with experimental matter radii.

Substituting the values (18) into our expressions for the matrix elements we obtain the following value of the matrix element $\langle 2s|W_{sp}|1p\rangle_{HALO}$

$$\begin{aligned} \langle 1p|W_{sp}|2s\rangle_{HALO} &= -i0.2 \quad g_n^W \quad eV, \\ &= -i0.2 \quad eV \quad (for \quad g_n^W \simeq 1 \quad). \end{aligned} \tag{19}$$

It is seen that this value is only few times smaller than the standard value of the matrix element of the weak potential between the opposite parity states in spherical nuclei (see e.g., [2]), that is typically about one eV. This results from the wave function structure and comes basically from the facts that the $2s$ wave function crosses zero line near the core surface while the $1p$ radial wave function does not have nodes. Thus the functions χ_{1p} and $d\chi_{2s}/dr$ look similar and are folded constructively with $\rho_c(r)$ in the region of interaction (nuclear interior), see Fig.6.

The matrix element of W_{sp} between the "normal" nuclear states can be evaluated for example, in the oscillator model. Taking the typical matrix element between the states $2s$ and $1p$ and using the same formula (14), one has

$$\langle 1p|W_{sp}|2s\rangle_{osc} = -ig_n^W G\rho_0 \left(\frac{\omega}{2m}\right)^{1/2} \tag{20}$$

where $\omega \simeq 40A^{-1/3} MeV$ is the oscillator frequency [32] with A the nuclear mass number. We used here the constant value of the core nucleon density, $\rho_0 \simeq 0.138 fm^{-1/3}$. This is very good approximation in the case of normal nucleus [25].

Recalling the energy difference between the ground state and the first excited state $1p$ that is known experimentally,

$$|\Delta E_{HALO}| = E_{p1/2} - E_{s1/2} = 0.32 MeV \tag{21}$$

we obtain, using Eq.(19), the coefficient of mixing the opposite parity state ($1p$) to the halo ground state $2s$:

$$|f_{sp}^{HALO}| = \frac{|\langle 1p|W_{sp}|2s\rangle|}{|\Delta E_{HALO}|} \simeq \frac{0.2eVg^W}{0.32MeV}$$
$$\simeq 0.6\times 10^{-6} g_n^W$$
$$\simeq 0.6\times 10^{-6} \quad (for \quad g_n^W \simeq 1) \tag{22}$$

This PNC mixing is about one order of magnitude stronger than the scale of single-particle PNC mixing in "normal" nuclear states that can be extracted from Eq.(20). In the case of normal $p-s$ mixing, we have

$$|f_{sp}^{normal}| = \frac{|\langle 1p|W_{sp}|2s\rangle|}{\omega} = \frac{Gg_n^W\rho_0}{\sqrt{2}m}\left(\frac{m}{\omega}\right)^{1/2}$$
$$\simeq 0.7\times 10^{-7} g_n^W$$
$$\simeq 0.7\times 10^{-7} \quad (for \quad g_n^W \simeq 1) \tag{23}$$

in the same region of nuclei with $A\sim 11$. The above value (23) for the normal PNC mixing is rather universal and it is practically insensitive to variations of the details of the normal nuclear wave functions and core densities [25]. One should stress that in the halo case, the energy denominator in Eq.(22) is $\omega/|\Delta E_{HALO}| \simeq 50$ times smaller than in the normal case (23) based on the oscillator model. Comparing Eqs.(22) and (23), we find the halo enhancement factor in the PNC mixing to be

$$\frac{|f_{sp}^{HALO}|}{|f_{sp}^{normal}|} \simeq 9. \tag{24}$$

This result is quite remarkable in a number of respects. First, it is seen that in experiments when the halo wave functions in nuclear exterior are probed, the value of PNC mixing is even stronger than in "normal" nuclei. Secondly, this PNC mixing is dominated by the neutron weak constant g_n^W. Such experiments with neutron halo nuclei would therefore provide unique opportunity to probe the value of this constant. Usually, sensitivity of experiments to the value of this constant is "spoiled" by comparably large value of the proton weak constant g_p^W, cf. Eqs. (7).

In order to assess reliability of the results, we have studied stability of the enhancement factor against variations in the parameters of the halo wave functions. As one can see from the results presented in Table I, the matrix element (19) is changed by few per cent only when the wave functions are deformed. The enhancement factor (22) is therefore quite stable.

VI. CONCLUSION

Having in mind to present a first estimate of the PNC effect in halo nuclei, we have chosen here the simplest possible case of one-body halo where the existing data allow one to rely on simple analytical model of halo structure. In this work, we confined ourselves to the case of exotic nucleus ^{11}Be for which we presented detailed consideration.

The analysis presented above rests basically on the most reliably known facts: the quantum numbers of the states involved, the halo radii which match the matter radii known from experiment, and the Hartree-Fock wave functions. With these input data, the further quantitative analysis is a straightforward analytical exercise which does not require any approximations. Stability of the results has been checked analytically. The PNC enhancement factor of one order of magnitude allows one to to speak about qualitative halo effect that should not be overlooked.

It is the matter of further studies to check universality of the effect while going along the table of exotic nuclei. One sees that other exotic nuclei with developed halo structure manifest similar properties (see, e.g., [12]). Indeed, the effect of PNC enhancement found here results basically from the two facts:

(i) small energy separation between the mixed opposite parity states

(ii) considerably strong overlap between the mixed wave functions and the core density, which saves part of suppression in the PNC weak matrix element.

The first of these points is rather common for nuclei with developed neutron halos. Systematics of separation energies for single neutron [13] shows that the ground states of halo nuclei can be distanced from the continuum by typical spacing $\varepsilon_{halo} \sim (2mr_{halo})^{-1/2} \sim$ few hundreds of KeV. Even in the cases when no bound states with parity opposite to that of the ground state occur, the PNC admixtures to the ground state wave functions must exist. In these cases, the PNC admixtures can be evaluated by means of Green function method.

The second point (ii) is related to the wave function structure and requires further studies. It would be also interesting to study the PNC effects in proton rich nuclei [19], [20], [21].

One should mention that the results obtained here are based on the single-particle approximation (one-body halo model). In principle, the halo neutron can couple to excitations of the core (see, e.g. [33]). In fact, such coupling can be responsible for the small energy separation between the opposite parity levels in ^{11}Be, which can be separated by few MeV otherwise (see, e.g., [22]). These many-body effects may be important for precise evaluation of the PNC mixing, which is beyond the scope of this paper. We did not consider contribution from such effects here.

In conclusion, we have shown in this work that the ground state of exotic nuclei with developed halo structure contain mixing of parity violating admixtures of opposite parities, using the nucleus ^{11}Be as a representative case. Originating at the core scale, where the halo wave functions overlap strongly with the core nucleon wave functions, these PNC admixtures can manifest themselves in the nuclear exterior, where the halo neutron wave functions contain admixtures that are about one order of magnitude bigger than in the case of normal nuclear states. Such PNC admixtures can be tested in experiments that can probe halo wave functions in nuclear exterior. Moreover, it is important that the PNC admixtures in neutron halo are sensitive to the neutron weak constant g_n^W, thus providing a new interesting possibility to probe this weak constant whose value is the most doubtful point of the present theory of PNC weak interaction.

One of possible experimental manifestations of the discussed effect is related to anapole moment [23], [24] which attracts much attention in current literature [30] in view of new experimental results (detection of anapole moment in nucleus ^{133}Cs [31]). Since the anapole moment is created by the toroidal electromagnetic currents which results from PNC, its

value grows as the size of the system increased [24]. In the case of halo which we considered here, the value of the anapole moment can be therefore enhanced due to extended halo cloud. We hope to address these issues in following publications.

VII. ACKNOWLEDGEMENT

The authors are grateful to V.V.Flambaum for discussions of of issues related to PNC effects. The work has been supported by FAPESP (Fundacao de Amparo a Pesquisa do Estado de Sao Paulo) and in part by funds provided by the U.S. Department of Energy (D.O.E.) under contract #DE-FC02-94ER40818.

REFERENCES

[1] B.Desplanques, J. Donoghue, and B.Holstein, Ann. Phys. (N.Y.) **124**,449 (1980).
[2] E.G.Adelberger and W.C.Haxton, Ann. Rev. Nucl. Part. Sci. **35**, 501 (1985).
[3] J.D.Bowman, C.D.Bowman, J.E.Bush, P.P.J.Delheij, C.M.Frankle, C.R.Gould, D.G.Haase, J.Knudson, G.E.Mitchel, S.Penttila, H.Postma, N.R.Robertson, S.J.Seestrom, J.J.Szymansky, V.W.Yuan, and X.Zhu, Phys.Rev.Lett. **65**, 1192 (1990).
[4] M.B.Johnson, J.D.Bowman, and S.H.Yoo, Phys.Rev.Lett. **67**, 310 (1991).
[5] O.P. Sushkov and V.B. Telitsin, Phys.Rev. **C48**, 1069 (1993).
[6] B. Desplanques, Phys. Rep. **297**, 1 (1998).
[7] W.S. Wilburn and J.D. Bowman, Phys. Rev. **C57**, 3425 (1998).
[8] D.B. Kaplan, M.J. Savage, R.P. Springer, and M.B. Wise, Phys.Lett. **B449**, 1 (1999).
[9] H.Feshbach, M.S.Hussein, A.K. Kerman, and O.K.Vorov, to appear in Adv. Nucl. Phys.
[10] J.S. Al-Khalili and J.A. Tostevin, Phys.Rev.Lett. **76**, 3903 (1996).
[11] R.C. Johnson, J.S. Al-Khalili, and J.A. Tostevin, Phys.Rev.Lett. **79**, 2771 (1997).
[12] H. Sagawa, Phys. Lett. **B286**, 7 (1992).
[13] C.A. Bertulani, L.F.Canto, and M.S.Hussein, Phys. Rep. **226**, 281 (1993).
[14] C.A. Bertulani, L.F.Canto, and M.S.Hussein, Phys. Lett. **B353**, 413 (1995).
[15] K.Hencken, G.Bertsch and H.Esbensen Phys. Rev **C54**, 3043 (1996).
[16] A. Mengoni, T. Otsuka, T. Nakamura, and M. Ishihara, Contribution to the 4th International Seminar on Interaction of Neutrons with Nuclei, Dubna (Russia), April 1996, Preprint nucl-th/9607023.
[17] J.Hardy, talk given at Int. Workshop on Physics of Unstable Nuclear Beams, Serra-Negra (Brazil) 1996.
[18] T. Suzuki, In *Physics of Unstable Nuclear Beams*, C.A.Bertulani, L.F.Canto, and M.S.Hussein ed., World Scientific, Singapore, 1997, p.157.
[19] B.A. Brown and P.G. Hansen, Phys.Lett. **381B**, 391 (1996)
[20] S. Karataglidis and C. Bennhold, Phys. Rev. Lett. **80**, 1614 (1998).
[21] Z.Z. Ren, A. Faessler, and A. Bobyk, Phys.Rev. **C57**, 2752 (1998).
[22] H. Sagawa and K. Yazaki, Phys.Lett. **B244**, 149 (1990).
[23] Ya.B. Zel'dovich, Zh.Exp.Teor.Fiz. **33**, 1531 (1957) [Sov. Phys. JETP **6**, 1184 (1957)].
[24] V.V.Flambaum and I.B.Khriplovich, Zh.Eksp.Teor.Fiz. **79**,1656(1980) [Sov.Phys. JETP **52**, 835(1980)]; V.V.Flambaum and I.B.Khriplovich and O.P.Sushkov, Phys.Lett. **B146**, 367 (1984).
[25] V.F. Flambaum and O.K. Vorov, Phys.Rev.Letts. **70**,4051 (1993).
[26] V.F. Flambaum and O.K. Vorov, Phys.Rev. **C51**, 1521 (1995).
[27] N. Auerbach and B.A.Brown, Phys. Lett. **B340**, 6 (1994).
[28] W.C.Haxton, E.M.Henley, and M.J.Musolf, Phys.Rev.Lett. **63**, 949(1989).
[29] C.Bouchiat and C.A.Piketty, Z.Phys. **C49**, 91 (1991).
[30] W.Haxton, Science, **275**, 1753 (1997).
[31] C.S. Wood, S.C.Bennet, D.Cho, B.P.Masterson, J.L.Roberts, C.E.Tanner, and C.E. Wieman, Science **275**, 1759 (1997).
[32] A. Bohr and B. Mottelson, *Nuclear Structure* (Benjamin, New York, 1969), Vol. 1.
[33] T.T.S. Kuo, F. Krmpotic, and Y. Tzeng, Phys.Rev.Lett. **78**, 2708 (1997).

TABLES

TABLE I. Stability analysis for the matrix element of W_{sp} between the halo states $2s_{1/2}$ and $1p_{1/2}$. The results for the values of the parameters r_0 and r_1 differing from the best values are shown. The central entry in the table corresponds to the best value. It is seen that variations in r_0 and r_1 do not affect $\langle 2s_{1/2}|W_{sp}|1p_{1/2}\rangle$ any considerably.

	$r_0 = 1.40$	$r_0 = 1.45$	$r_0 = 1.50$
$r_1 = 1.75$	1.168	1.052	0.950
$r_1 = 1.80$	1.110	1.000	0.903
$r_1 = 1.85$	1.056	0.952	0.860

Figure Captions

Fig.1. a) Schematic plot of matter distribution in halo nuclei. The dark region corresponds to the nuclear core, the grey region shows the halo neutron cloud.

b) The spectrum of the bound states ^{11}Be.

c) Illustration of the single-particle PNC mixing in the ground state of ^{11}Be.

Fig.2. The core density distribution (logarithmic scale). The dashed line corresponds to Ref. [12], the solid line gives parametrization (15).

Fig3. The halo density in the ground state, $\rho_{2s1/2}(r) = \frac{1}{4\pi}\left(R_{2s1/2}(r)\right)^2$. The dashed line corresponds to the Hartree-Fock calculations of Ref. [12], the solid line gives parametrization (10),(18).

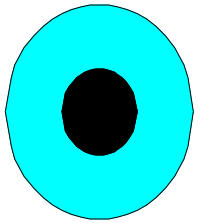
Fig.4. The halo density in the first excited state, $\rho_{1p1/2}(r) = \frac{1}{4\pi}\left(R_{1p1/2}(r)\right)^2$. The dashed line corresponds to the Hartree-Fock calculations of Ref. [12], the solid line gives parametrization (12),(18).

Fig.5. Plot of the radial wave functions of the states $|2s1/2\rangle$ and $|1p1/2\rangle$, $\chi_{2s1/2}(r) = rR_{2s1/2}(r)$ and $\chi_{1p1/2}(r) = rR_{1p1/2}(r)$.

Fig.6 . Plot of the functions contributing to the weak PNC matrix element. The function $s(r) = \frac{d}{dr}\chi_{1p1/2}(r) + \frac{\chi_{1p1/2}(r)}{r} + \frac{d\rho_c/dr}{2\rho_c}\chi_{1p1/2}(r)$ (dot-dashed line) depends on r in the way similar to $\chi_{2s1/2}(r)$ (dashed line). The combination $\chi_{2s1/2}(r)\rho_c s(r)$ that enters the PNC matrix element in Eq.(14) is shown by the solid line. It contributes coherently to $\langle 2s|W_{sp}|1p\rangle$.

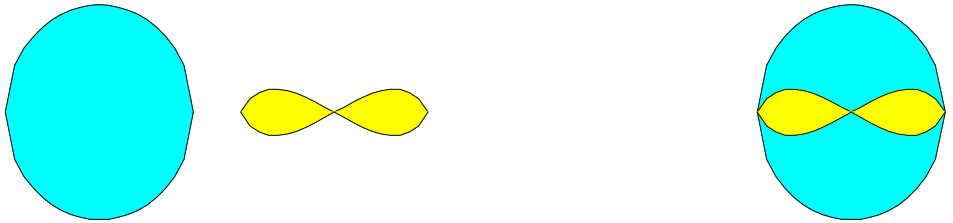
a)

b)





c)



2s 1p Ψ'

Fig. 2

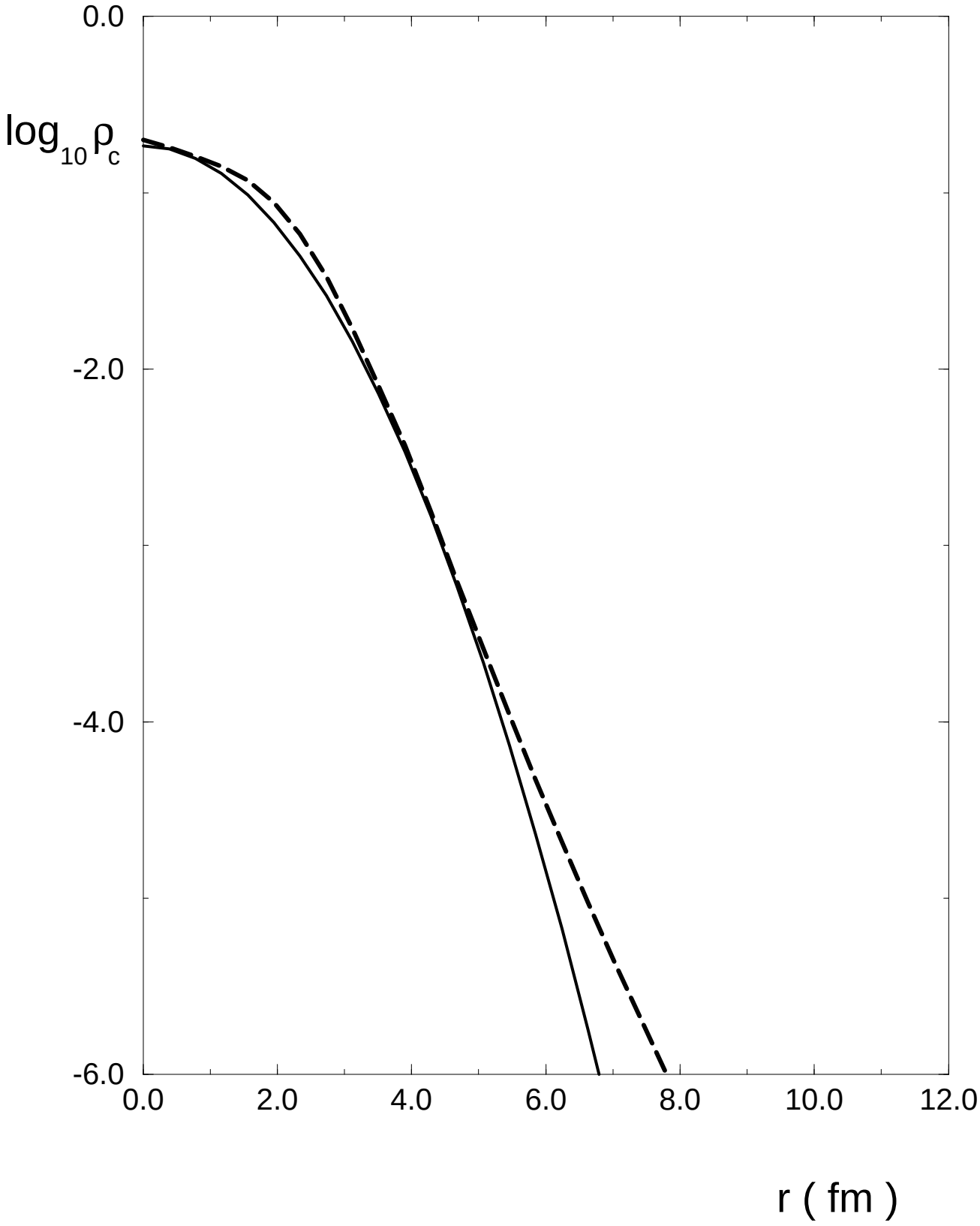


Fig. 3

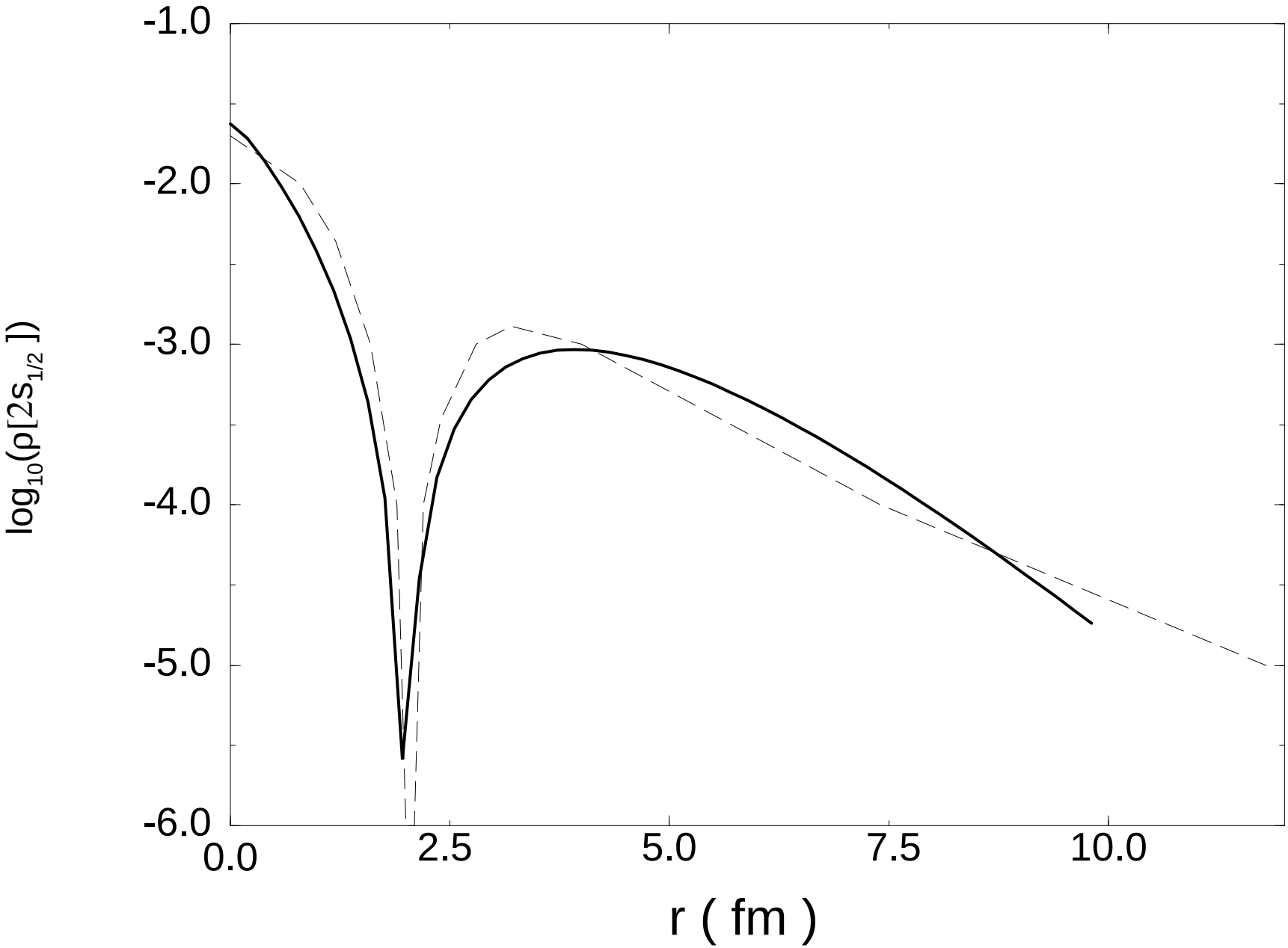
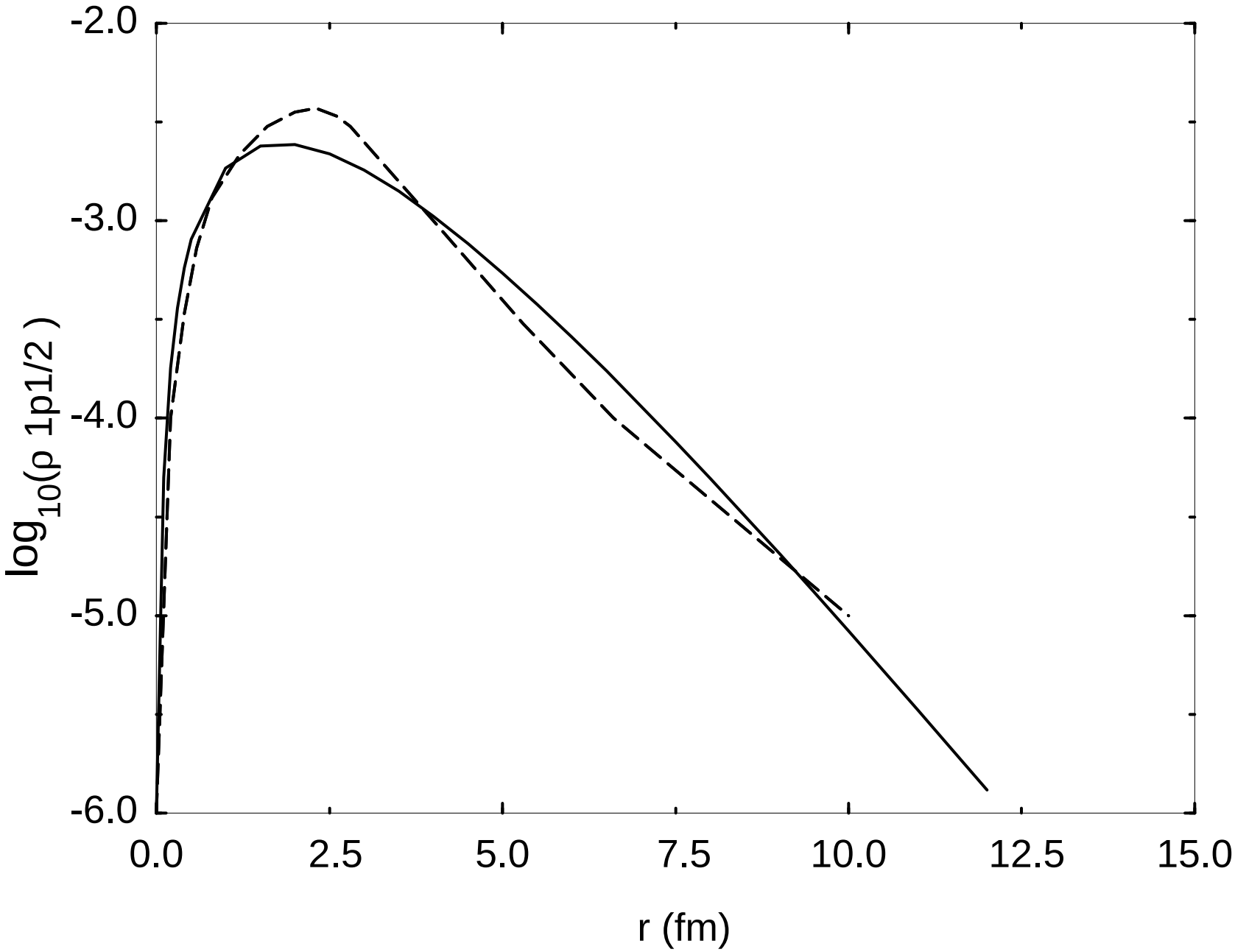


Fig. 4



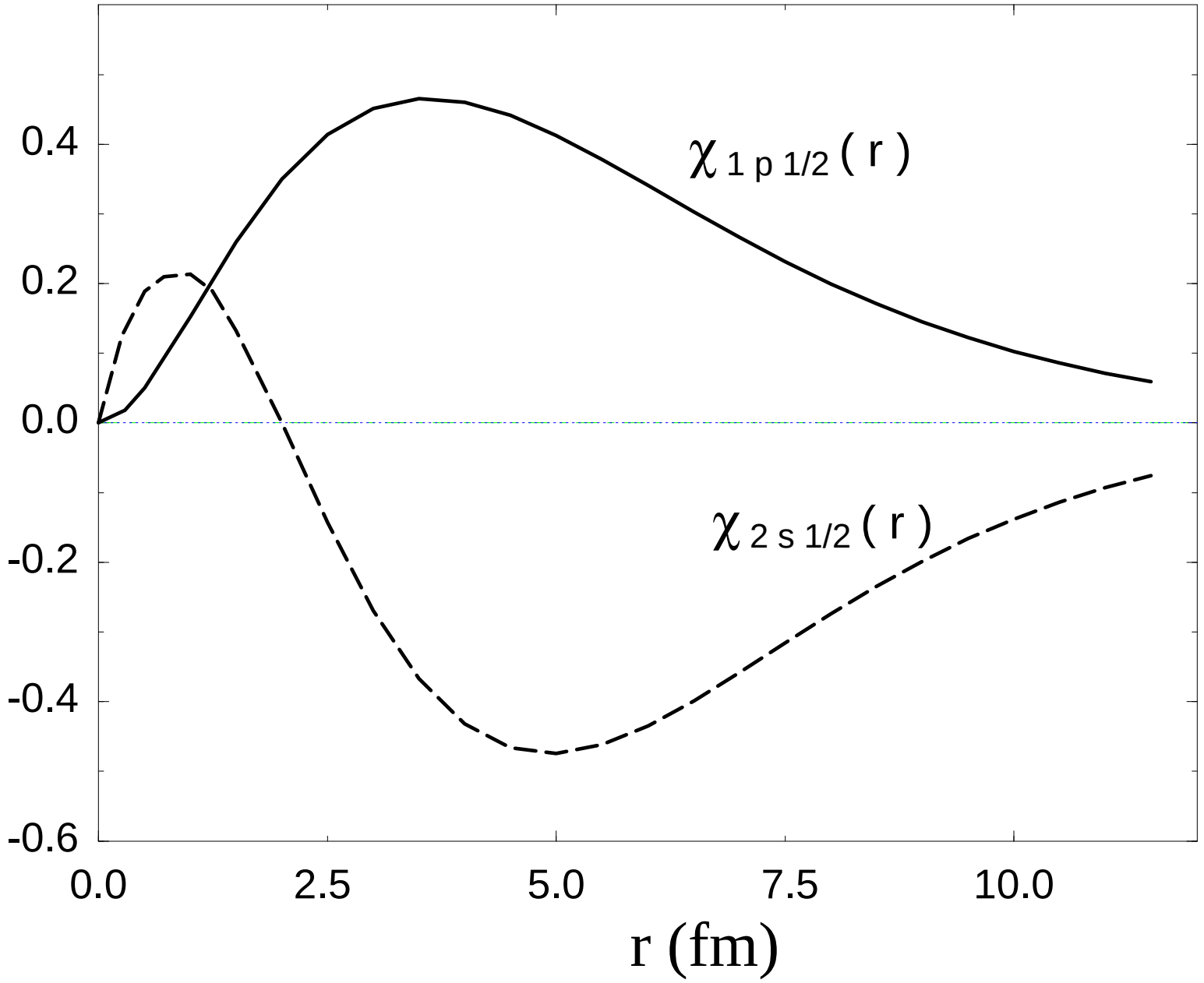

0.4
0.2
0.0
-0.2
-0.4
-0.6
0.0
2.5
5.0
7.5
10.0
r (fm)
χ 1 p 1/2 (r)
χ 2 s 1/2 (r)

Fig. 6

